Nonlinear Atomic Response to Intense Ultrashort X Rays

G. Doumy,[1,2] C. Roedig,[1] S.-K. Son,[3] C. I. Blaga,[1] A. D. DiChiara,[1] R. Santra,[3,4] N. Berrah,[5] C. Bostedt,[6] J. D. Bozek,[6] P. H. Bucksbaum,[7] J. P. Cryan,[7] L. Fang,[5] S. Ghimire,[7] J. M. Glownia,[7] M. Hoener,[5] E. P. Kanter,[2] B. Krässig,[2] M. Kuebel,[8] M. Messerschmidt,[6] G. G. Paulus,[8] D. A. Reis,[7] N. Rohringer,[9] L. Young,[2] P. Agostini,[1] and L. F. DiMauro[1]

[1]*The Ohio State University, Columbus, Ohio 43210, USA*
[2]*Argonne National Laboratory, Argonne, Illinois 60439, USA*
[3]*Center for Free-Electron Laser Science, DESY, 22607 Hamburg, Germany*
[4]*Department of Physics, University of Hamburg, 20355 Hamburg, Germany*
[5]*Western Michigan University, Kalamazoo, Michigan 49008, USA*
[6]*Linac Coherent Light Source, SLAC National Accelerator Laboratory, Menlo Park, California 94025, USA*
[7]*Stanford PULSE Institute, SLAC National Accelerator Laboratory, Menlo Park, California 94025, USA*
[8]*Institute of Optics and Quantum Electronics, 07743 Jena, Germany*
[9]*Lawrence Livermore National Laboratory, Livermore, California 94551, USA*

(Received 13 December 2010; published 24 February 2011)

The nonlinear absorption mechanisms of neon atoms to intense, femtosecond kilovolt x rays are investigated. The production of Ne^{9+} is observed at x-ray frequencies below the Ne^{8+}, $1s^2$ absorption edge and demonstrates a clear quadratic dependence on fluence. Theoretical analysis shows that the production is a combination of the two-photon ionization of Ne^{8+} ground state and a high-order sequential process involving single-photon production and ionization of transient excited states on a time scale faster than the Auger decay. We find that the nonlinear direct two-photon ionization cross section is orders of magnitude higher than expected from previous calculations.

DOI: 10.1103/PhysRevLett.106.083002 PACS numbers: 32.80.Rm, 42.55.Vc, 42.65.Re, 52.59.−f

The invention of the optical laser enabled the first observation of second harmonic generation by Franken and co-workers [1] in 1961, thus opening the field of nonlinear optics. The study and application of nonlinear processes from the microwave to the ultraviolet frequencies is extensive and well documented. Recently, those studies have been extended to the extreme ultraviolet (XUV) photon energy range, first with high harmonics sources [2], and then with XUV free-electron lasers [3]. Nonlinear investigations in the x-ray regime have, to date, remained purely a theoretical pursuit. One reason for the absence of experiments is the rapid decrease of nonlinear susceptibility with increasing frequency ν. This can be seen by considering a perturbative two-photon transition whose cross section $\sigma^{(2)}$ can be approximated as $\sigma^{(1)}\tau\sigma^{(1')}$, where $\sigma^{(1)}$ and $\sigma^{(1')}$ are one-photon cross sections and τ is the reciprocal of the detuning [4]. For the nonresonant case, $\sigma^{(1)}$ and $\sigma^{(1')}$ can be assumed equal and $\tau \propto \nu^{-1}$, or, equivalently, the virtual state lifetime is the optical period. Consequently, passing from the visible frequencies to kilovolt x rays results in at least a 1000-fold decrease in $\sigma^{(2)}$, thus requiring higher intensity. The emergence of x-ray free-electron lasers (XFEL) capable of producing intense, kilovolt x rays enables the first experimental steps towards developing nonlinear short-wavelength optics, that will ultimately extend to condensed-phase samples, for which x rays are ideal due to their much larger penetration length and much greater element specificity when compared to lower frequency radiation.

This Letter reports an experimental study on the nonlinear ionization of neon atoms with intense x rays above 1 keV photon energy using the Linac Coherent Light Source (LCLS) XFEL at the SLAC National Accelerator Laboratory. Ion yield measurements performed as a function of x-ray pulse energy and frequency reveal a dependence consistent with a nonlinear process. Several mechanisms are treated in a theoretical model that produces good agreement with the observed ion distributions. Two contributing nonlinear processes competing on the Auger time scale are considered: two-photon, one-electron direct ionization and two-photon, two-electron sequential ionization involving transient excited states.

The LCLS XFEL produces $\sim 10^{13}$ photons in a $\sim$100 fs burst over a 560–10 000 eV photon energy range (or 1.2–22 Å) [5], at a 120 Hz repetition rate (originally at 30 Hz). The experiments utilized the high-field instrumentation of the Atomic, Molecular and Optical Science (AMOS) end station, which is capable of producing a focused x-ray beam (0.8–2 keV) with a peak intensity of $\sim 10^{17}$ W/cm^2. This unprecedented capability for producing electric fields in excess of an atomic unit [6] enables nonlinear x-ray studies. In the x-ray regime, the nonlinearities will be dominated by core electrons in contrast to valence excitation at optical frequencies. This results in some obvious physical differences: (1) the excited state is a core vacancy, (2) the x-ray excitation rate must compete with rapid atomic relaxation, e.g., Auger, and (3) several electronic states can contribute.

In our experiment, neon is used since K- and L-shell ionization is accessible with the AMOS beam line photon energy range. Previous studies [7,8] have shown that the high fluence LCLS x rays produce in a single pulse highly charged neon ions through a series of one-photon absorption and relaxation (Auger and fluorescence) processes (see, e.g., Fig. 1 in Ref. [8]). This allowed us to study the possibility of direct two-photon ionization of helium-like neon, Ne^{8+}. We used 2 different photon energies, above (1225 eV) and below (1110 eV) the Ne^{8+} K-shell threshold at 1196 eV. As depicted in Fig. 1(a), Ne^{9+} can be produced by one- or two-photon absorption, respectively. Consequently, above the edge, a linear dependence on fluence results for the Ne^{9+}/Ne^{8+} ratio, while below this energy a quadratic response is expected. The photon energy below the edge was chosen so that it is still above Ne^{6+} K-shell ionization energy (1096 eV) (to efficiently produce Ne^{8+} target through a sequence of $1s$ ionizations and Auger decays), but below the K-shell edge of Ne^{7+} to try to minimize pathways for the production of Ne^{9+} that do not include the ground state Ne^{8+} (see Fig. 5 in Ref. [7]).

Ionic charge state distributions are measured using a Wiley-McLaren time-of-flight ion spectrometer. The pulse energy is measured independently by a calibrated gas detector [9] and controlled using a variable-pressure N_2 gas attenuator cell. The pulse duration is inferred from the measured electron bunch duration. The spectrometer data, as well as other LCLS and end-station diagnostic information, e.g., electron beam energy, x-ray energy, are recorded for each x-ray pulse, which allows for postexperiment sorting.

Critical for observing a nonlinear direct two-photon absorption, similar to that illustrated in Fig. 1(a), is a high intensity x-ray beam that is free of harmonic spectral contamination. The high intensity condition is easily satisfied by tight focusing of the x-ray beam ($\sim 2\ \mu m^2$) using a Kirkpatrick-Baez (KB) mirror pair. The x-ray fluence on target was determined using theoretical calculations to match the neon ions' charge state distributions [8]. Details on the modeling follow further in the text. Our analysis shows that the fluence on target is $\sim 15\ kJ/cm^2$, for a 1.5 mJ pulse, or, alternately, an intensity of $2 \times 10^{17}\ W/cm^2$ for a pulse of 100 fs duration.

The harmonic spectral content of the x-ray beam, inherent to saturated FEL operation, is a more challenging issue for a nonlinear measurement. Accordingly, the AMOS beam line was designed to minimize this radiation by using boron carbide optics (transport and KB mirrors) that have a cutoff at 2 keV [10]. The optics reflectivity effectively reduces the third-harmonic content (1% of the total energy) over the full tuning range (0.8–2 keV), but the weaker second harmonic ($\sim 0.01\%$) is more problematic [11]. All the reported measurements were safely conducted above 1.1 keV photon energy where the optics provide $>10^2$ additional harmonic suppression, thus reducing the second-harmonic content to less than 10^{-6} with respect to the fundamental beam.

Figures 2(a) and 2(b) show the measured charge state distributions (black bars) at the 2 photon energies. Clearly Ne^{9+} is observed in both cases although with less abundance ($\sim 1\%$) below threshold, as opposed to $\sim 10\%$ above

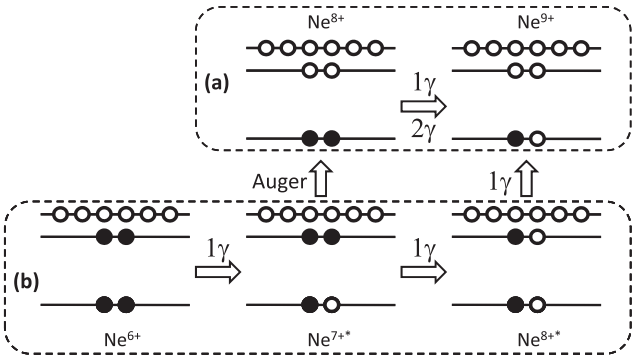

FIG. 1. Illustration of Ne^{9+} production. (a) Direct process through one-photon (1γ) or two-photon (2γ) ionization of Ne^{8+}, depending on the photon energy. (b) Indirect process first ionizes Ne^{6+} into Ne^{7+*} excited state. Before Auger decay occurs, which would otherwise direct through (a), a valence electron is photoionized to produce Ne^{8+*} that can also be subsequently ionized into Ne^{9+}.

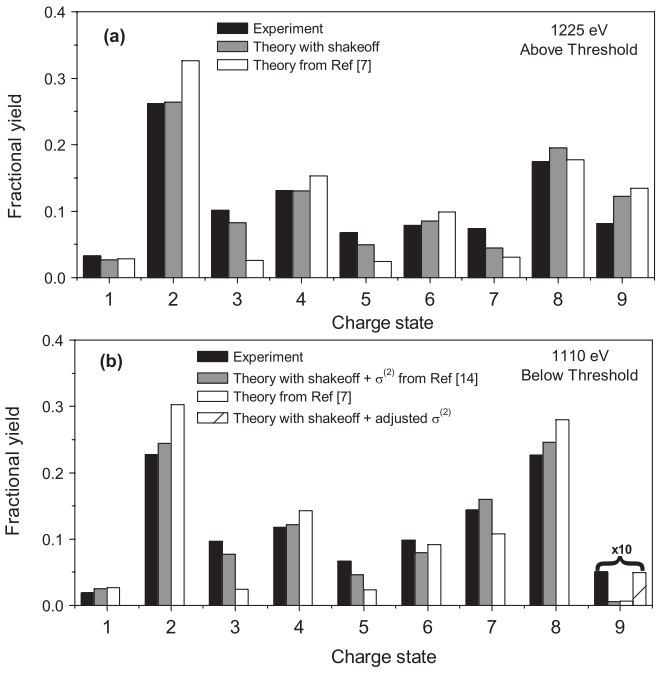

FIG. 2. Charge state distributions produced by (a) 1225 eV (1.45 mJ) and (b) 1110 eV (1.27 mJ) beams. Black: experiment (the detection efficiency for the different charge states is adjusted using the procedure of Ref. [8]). White: model used in Ref. [7]. Gray: improved model accounting for shakeoff processes. The striped bar in (b) incorporates the adjusted $\sigma^{(2)}$ needed to reproduce the Ne^{9+} production below threshold.

threshold. Since one-photon ionization of the Ne^{8+} ground state is a closed channel below threshold, Ne^{9+} production must involve a higher-order process. Additional insight can be obtained by studying the dependence of the Ne^{9+}/Ne^{8+} ratio as a function of pulse energy, as plotted in Fig. 3 for both photon energies. To facilitate comparison the ratios are normalized to unity for an incident pulse energy of 0.8 mJ. The different rates for the Ne^{9+}/Ne^{8+} ratio as a function of pulse energy are evident: quadratic below and linear above threshold. The quadratic dependence below threshold is indicative of a two-photon absorption process and rules out any significant contribution of one-photon (linear) absorption caused by second-harmonic contamination.

We performed theoretical calculations in order to identify the origin of the nonlinear mechanism(s) amongst the succession of competing one-photon processes, as well as provide an additional constraint on the fluence. A simple rate equation model has been shown to reproduce the main features in the measured charge distributions [8]. The model is based on one-photon absorption cross sections and atomic relaxation rates obtained with a conventional Hartree-Fock-Slater approach [7] and incorporates spatial and temporal averaging. Not unexpected for a linear absorption model, the averaged calculated ion distribution is insensitive to the detailed XFEL pulse shape, e.g., spikey FEL temporal structure due to the chaotic process [5]. The results of the model of Ref. [7] used in Ref. [8] are presented in Fig. 2 and show good overall agreement except that it predicts a stronger alternation in the odd-even charge state amplitudes than measured and thus underestimates the odd-charge state yield.

To improve our understanding, and specifically the Ne^{9+} production below threshold, the model was modified to include shakeoff processes as well as direct two-photon ionization of Ne^{8+}. Previous synchrotron studies have shown that a significant fraction ($\sim 25\%$) of Ne^{3+} is formed via shakeoff from neutral K-shell ionization [12]. The single and double shakeoff branching ratios following K-shell ionization were calculated using the Hartree-Fock-Slater method within the sudden approximation [13]. In addition, a two-photon cross section (10^{-56} cm^4 s) for Ne^{8+} ionization was adopted from the calculations of Novikov and Hopersky [14]. Other nonlinear processes are expected to have a weak contribution to the Ne^{9+} production and were neglected. The modified model (gray bars in Fig. 2) significantly improves the agreement with the experiment for both photon energies; e.g., the strong alternation in the odd-even charge state distributions is reduced. It further establishes with better than 20% accuracy the fluence on target. However, significant discrepancies remain for the Ne^{9+} production at both photon energies: overestimated at 1225 eV and underestimated at 1110 eV.

The *absolute* value of the Ne^{9+}/Ne^{8+} ratio (a) above and (b) below threshold, calculated with this modified model (solid line), is compared to the experiment in Fig. 4. Above threshold (1225 eV), the linear variation (one-photon ionization of Ne^{8+}) is well reproduced, except near saturation for the highest pulse energies, but the model overestimates the ratio by 40% for all pulse energies. Below threshold (1110 eV) the agreement is poorer: although the quadratic behavior is reproduced, it severely underestimates the Ne^{9+} yield by an order of magnitude. In addition, the ratio predicted using only the two-photon

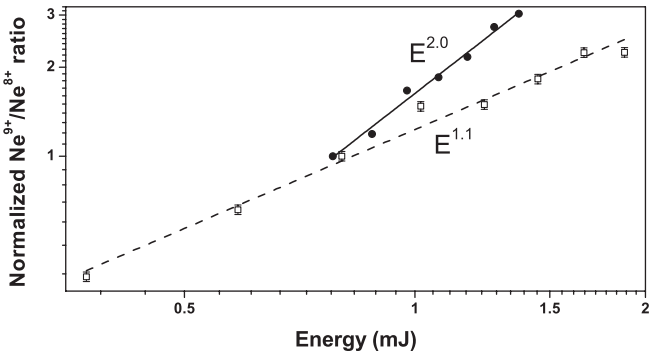

FIG. 3. Normalized Ne^{9+}/Ne^{8+} ratio as a function of pulse energy for 1110 eV (filled circles) and 1225 eV (open squares). Fits yield a quadratic response at 1110 eV (solid line) and linear behavior at 1225 eV (dashed).

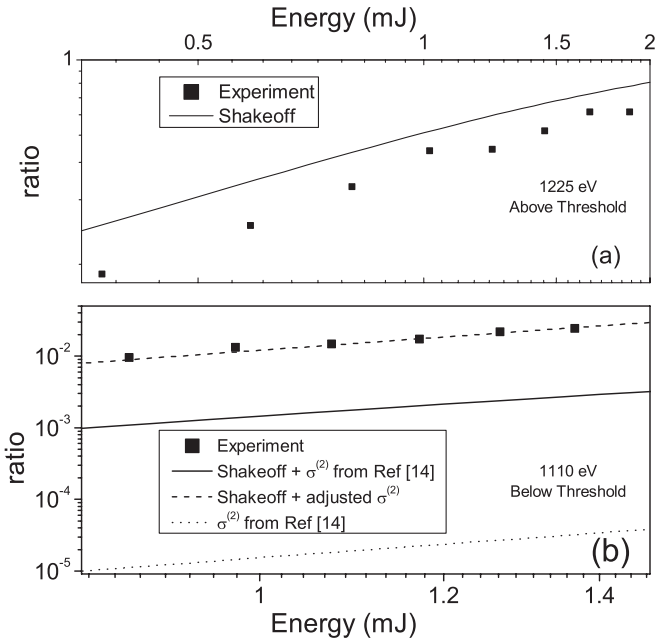

FIG. 4. The measured absolute Ne^{9+}/Ne^{8+} ratio (symbols) as a function of x-ray pulse energy is compared with the modified model (solid line), incorporating shakeoff and *direct* two-photon ionization of Ne^{8+} using $\sigma^{(2)}$ from Ref. [14], (a) above and (b) below the Ne^{8+} one-photon threshold. In (b), the dotted line isolates the direct two-photon contribution, derived by subtracting results with and without $\sigma^{(2)}$ from Ref. [14]. The dashed line is a result of the enhanced $\sigma^{(2)}$ value (see text).

cross section of Ref. [14] (dotted line) has a negligible contribution to the total calculated ratio and underestimates the experiment by 3 orders of magnitude.

The modified model suggests then first the existence of an alternate pathway to production of Ne^{9+} below threshold that involves only one-photon absorption processes. The identity of this mechanism is depicted in Fig. 1(b), as a sequence of energetically open one-photon channels. The process is initiated by K-shell ionization of Ne^{6+} resulting in a long-lived (up to ~60 fs [15]) excited hole state of Ne^{7+*}. The highest probability path is Auger decay into $1s^2$ configuration; thus, the measured Ne^{8+} is almost equal to the transient Ne^{7+*} population. However, the high XFEL fluence and long Auger lifetime makes valence ionization also possible (~ 10%), thus forming a metastable excited $1s2s$ configuration of Ne^{8+*}. At 1110 eV, the $1s2s$ K-shell ionization is closed; thus, only valence ionization can produce Ne^{9+}. Under our experimental conditions, the model [solid line in Fig. 4(b)] recovers a quadratic response since the rate-limiting step is the two sequential one-photon absorptions by two valence electrons that have similar cross sections originating with Ne^{7+*} $[1s^1\ 2(s, p)^2]$ configuration.

The very good agreement with experiment for $q \leq 8$ finally suggests other shortcomings to explain the discrepancies with the measured Ne^{9+} production. Above threshold, it could come from the neglect of resonant excitation for different ionic species. That is, the $1s^12s^2 \rightarrow 1s^02s^25p^1$ resonance in Ne^{7+*} is near the 1225 eV excitation. Since the single-hole $(1s^12s^2)$ state is the critical intermediate path to the formation of Ne^{9+} in Fig. 2(b), a competing resonant channel can deplete the Ne^{9+} production predicted by the model, thus yielding better agreement with the experiment. However, no similar resonant scenario exists at 1110 eV and thus one-photon higher-order processes underestimate the below threshold production of Ne^{9+}.

The only remaining element that can lead to Ne^{9+} is the *direct* two-photon cross section, $\sigma^{(2)}$, which was adopted from Ref. [14]. At 1110 eV, their $\sigma^{(2)}$ value (10^{-56} cm^4 s) is only slightly larger (~ 4 times) than a nonresonant value derived from simple perturbative scaling arguments [4]. Conversely, Novikov and Hopersky also showed that at lower energy $|1s^1(2, 3)p\rangle$ intermediate states can significantly increase the $\sigma^{(2)}$ value by 9 orders of magnitude on resonance. However, their calculation neglects the $|1s^14p\rangle$ state at a transition energy of 1127 eV [16]. The large bandwidth of the XFEL (~ 10 eV) should make this resonance relevant to the magnitude of the two-photon cross section at 1110 eV. In order to reproduce not only the slope but also the absolute value of the ratio Ne^{9+}/Ne^{8+} [Fig. 2 (striped bar) and Fig. 4 (dashed line)], a value of 7×10^{-54} cm^4 s has to be used for $\sigma^{(2)}$. Two factors will tend to lower this value: (1) the x-ray pulse may be shorter than the 100 fs electron bunch [8] and (2) the chaotic temporal intensity spikes caused by the XFEL's short longitudinal coherence time [7]. Both factors can contribute no more than a factor of 2 reduction in $\sigma^{(2)}$. Consequently, our investigation concludes that $\sigma^{(2)}$ for Ne^{8+} is 2–3 orders magnitude higher than Ref. [14] due to near resonance contributions.

In conclusion, neon atoms subjected to ultraintense, 1 keV x rays undergo a complex sequence of excitation, ionization, and relaxation processes. Our experiment combined with theoretical analysis has identified and characterized the nonlinear response resulting from two channels: (1) the dominant *direct* two-photon, one-electron ionization and (2) a sequence of transient excited states that competes with the Auger decay clock. As with the Franken experiment 50 years ago, it is expected that this observation coupled with future technical improvement will underpin the emergence of nonlinear x-ray physics.

Portions of this research were carried out at the LCLS at the SLAC National Accelerator Laboratory. LCLS is funded by the U.S. Department of Energy, Office of Basic Energy Sciences. The work was funded by the DOE/BES under Contracts No. DE-FG02-04ER15614, No. DE-AC02-06CH11357, No. DE-FG02-92ER14299, and No. DE-AC52-07NA27344. Research of P. H. B., D. A. R., J. M. G., J. P. S., and S. G. is supported through PULSE at SLAC by DOE/BES.

[1] P. A. Franken *et al.*, Phys. Rev. Lett. **7**, 118 (1961).
[2] Y. Kobayashi *et al.*, Opt. Lett. **23**, 64 (1998); N. Papadogiannis *et al.*, Phys. Rev. Lett. **90**, 133902 (2003).
[3] V. Richardson *et al.*, Phys. Rev. Lett. **105**, 013001 (2010); M. Richter *et al.*, *ibid.* **102**, 163002 (2009); A. Sorokin *et al.*, *ibid.* **99**, 213002 (2007); Phys. Rev. A **75**, 051402 (R) (2007).
[4] P. Lambropoulos and X. Tang, J. Opt. Soc. Am. B **4**, 821 (1987).
[5] P. Emma *et al.*, Nat. Photon. **4**, 641 (2010).
[6] The atomic unit of electric field is defined by Coulomb field in the ground state of the hydrogen atom and equals 51 V/ Å or an equivalent intensity of 3.5×10^{16} W/cm^2.
[7] N. Rohringer and R. Santra, Phys. Rev. A **76**, 33416 (2007).
[8] L. Young *et al.*, Nature (London) **466**, 56 (2010).
[9] S. Hau-Riege *et al.*, Phys. Rev. Lett. **105**, 043003 (2010).
[10] R. Soufli *et al.*, Proc. SPIE Int. Soc. Opt. Eng. 7361, 73610U (2009).
[11] D. Ratner *et al.*, in *Proceedings of the 32nd International Free Electron Laser Conference (FEL2010), Malmö, Sweden, 2010*, oraweb.cern.ch/pls/fel2010/toc.htm, paper TUOB4.
[12] N. Saito and I. Suzuki, Phys. Scr. **45**, 253 (1992).
[13] A. Kochur *et al.*, J. Phys. B **27**, 1709 (1994).
[14] S. Novikov and A. Hopersky, J. Phys. B **34**, 4857 (2001).
[15] C. Bhalla *et al.*, Phys. Rev. A **8**, 649 (1973).
[16] Yu. Ralchenko, A. E. Kramida, J. Reader, and NIST ASD TEAM, http://physics.nist.gov/asd.